Letter

Engineering holographic flat fermionic bands

Nicolás Grandi,[1,2,*] Vladimir Juričić,[3,4,†] Ignacio Salazar Landea,[1,‡] and Rodrigo Soto-Garrido[5,§]

[1]*Instituto de Física de La Plata - CONICET, C.C. 67, 1900 La Plata, Argentina*
[2]*Departamento de Física - UNLP, Calle 49 y 115 s/n, 1900 La Plata, Argentina*
[3]*Departamento de Física, Universidad Técnica Federico Santa María, Casilla 110, Valparaíso, Chile*
[4]*Nordita, KTH Royal Institute of Technology and Stockholm University, Hannes Alfvéns väg 12, 106 91 Stockholm, Sweden*
[5]*Facultad de Física, Pontificia Universidad Católica de Chile, Vicuña Mackenna 4860, Santiago, Chile*

(Received 4 January 2022; accepted 17 March 2022; published 15 April 2022)

In electronic systems with flat bands, such as twisted bilayer graphene, interaction effects govern the structure of the phase diagram. In this paper, we show that a strongly interacting system featuring fermionic flat bands can be engineered using the holographic duality. In particular, we find that in the holographic nematic phase, two bulk Dirac cones separated in momentum space at low temperature, approach each other as the temperature increases. They eventually collide at a critical temperature yielding a flattened band with a quadratic dispersion. On the other hand, in the symmetric (Lifshitz) phase, this quadratic dispersion relation holds for any finite temperature. We therefore obtain a first holographic, strong-coupling realization of a topological phase transition where two Berry monopoles of charge one merge into a single one with charge two, which may be relevant for two- and three-dimensional topological semimetals.

DOI: 10.1103/PhysRevD.105.L081902

I. INTRODUCTION

Flat electronic bands have recently attracted significant attention due to the experimental realization of twisted bilayer graphene [1,2]. They naturally promote interaction effects as dominant, leading to a rich landscape of possible strongly correlated phases [3]. Strongly interacting systems, however, may be prohibitively difficult to address within the traditional frameworks, such as perturbation theory. Furthermore, numerical methods are restricted to exact diagonalization due to the sign problem present in systems involving fermionic degrees of freedom.

Given the necessity of using a nonperturbative approach, the AdS/CFT correspondence, also known as holographic duality [4–6], has been broadly used to investigate strongly coupled systems. In the more general sense, this duality proposes an equivalence between systems described by strongly interacting quantum field theories and weakly coupled systems in a curved spacetime with an extra spatial dimension. As such, these holographic methods so far have been useful to gain qualitative insights on condensed matter systems, for instance, non-Fermi liquids, high T_c superconductors, and topological systems, among others [7–9]. Given that flat bands favor the effects of the strong electronic interactions, including the ensuing new quantum phases and phase transitions, it is then rather natural to apply the holographic duality to address the physics at strong coupling therein. In this context, it is worthwhile emphasizing that a Lifshitz geometry may be the natural setting for the construction of the holographic flat bands, given that, at least from a perturbative point of view, the scaling of the electronic density of states $[\rho(\varepsilon)]$ with energy (ε) in d spatial dimensions is tunable by the dynamical exponent (z), $\rho(\varepsilon) \sim |\varepsilon|^{\frac{d}{z}-1}$. It is then expected that a tunable dynamical exponent could yield an instability toward a symmetry broken phase, as in the model for multi-Weyl semimetal we have recently proposed [10], realizing a phase transition into a nematic phase, as also found in Ref. [11]. However, none of these holographic models feature the fermions in the bulk geometry that may in turn explicitly yield the holographic flat fermionic bands.

Here, we address this important problem by incorporating the fermions directly into the model of Ref. [10]. By computing the Green function in the background geometry, we show that the dispersion relation of the fermions indeed displays the flattening feature. In particular, we find that in the nematic phase (Fig. 1), two Dirac cones separated in

*grandi@fisica.unlp.edu.ar
†juricic@gmail.com
‡peznacho@gmail.com
§rodrigo.sotog@gmail.com

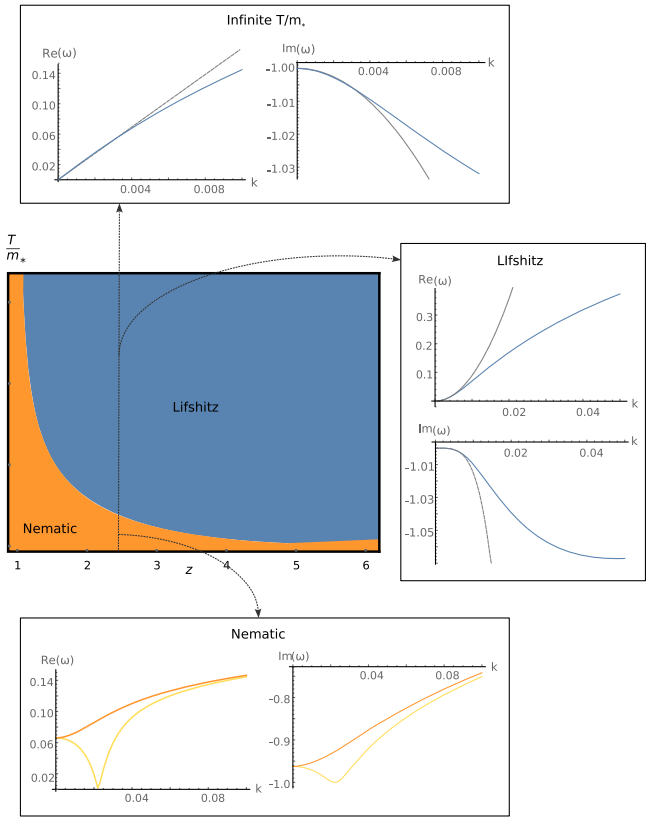

FIG. 1. Phase diagram of the model in Eq. (4), showing the nematic phase close to the origin and the Lifshitz one away from it. Top panel: the fermionic dispersion relation for infinite T/m_* (blue), with the dotted grey lines corresponding to the approximation in Eq. (16). Right-hand side panel: the dispersion corresponding to the Lifshitz phase for $T/m_* = 47.74$ (blue), with the grey lines corresponding to the approximation given by Eq. (17). Bottom panel: the anisotropic dispersion relation in the nematic phase, just below the critical temperature $T/m_* \approx 0.075$, along the two directions of Fig. 2. The yellow (orange) curve corresponds to the dispersion in the diagonal (antidiagonal) direction in momentum space, $\mathbf{k} = (k, k)$ [$\mathbf{k} = (k, -k)$]. We here set $q = q_D = 2$, i.e., $z = 2.48$.

momentum space at low temperature, approach each other as the temperature increases. Eventually, at the critical temperature, they collide yielding a flattened band with a quadratic dispersion relation, as shown in Fig. 2. On the other hand, in the symmetric (Lifshitz) phase, this quadratic dispersion relation holds for any finite temperature. Therefore, besides the holographic band flattening, we find a first holographic, strong-coupling realization of a topological phase transition where two Berry monopoles of charge one merge into a single monopole with charge two, which pertains to topological metals in both two [12–14] and three [15–18] spatial dimensions.

II. FREE MODEL

Let us first discuss the flat bands within a $(2+1)$-dimensional free Dirac fermion model. Our aim is to extract from it the symmetry breaking pattern that we will later export into the holographic realm. It is defined by the Hamiltonian

$$H'_D = -\gamma^t(\gamma^x p_x + \gamma^y p_y) \otimes \mathbb{1}_{2\times 2} + i m_*(\gamma^x \otimes \sigma_2 - \gamma^y \otimes \sigma_1), \tag{1}$$

where $\gamma^\mu = (\sigma_3, -i\sigma_2, i\sigma_1)$ are the Dirac gamma matrices, and the Pauli matrices σ_i in the second term act on an internal flavor index. This is analogous to the construction of the effective Hamiltonian for bilayer graphene by coupling two single layers each containing a linearly dispersing Dirac fermion. The spectrum reads

$$\omega = \pm m_* \pm \sqrt{p_x^2 + p_y^2 + m_*^2} \tag{2}$$

with gapped conduction and valence bands corresponding to both positive or both negative signs respectively, while otherwise the valence and conduction bands cross at zero energy. In the latter case, we obtain a low-energy $(p_x^2 + p_y^2 \ll m_*^2)$ quadratic dispersion

$$\omega \approx \pm \frac{1}{2m_*}(p_x^2 + p_y^2), \tag{3}$$

which still preserves rotational invariance.

The wave equation resulting from the Hamiltonian in Eq. (1) can be obtained from the action

$$S = S_{\text{free}} - i \int d^3x\, \bar{\Psi} \not{W} \Psi. \tag{4}$$

Here the first term is the free Dirac action for a pair of two-component spinors, while the deformation corresponds to a coupling of the pair to a constant non-Abelian vector field $W = m_*(\sigma^1 dx + \sigma^2 dy)$. This explicitly breaks the $U(2)$ symmetry down to the $U(1)$. Notice that spatial rotational invariance is also broken. However, there is a "mixed" rotational symmetry preserved in the system which is realized by compensating a spatial rotation with an internal transformation generated by σ_3. The latter is enough to preserve the rotational invariance of the spectrum.

III. HOLOGRAPHIC MODEL

We now construct a bottom up holographic dual to a strongly coupled version of the model in Eq. (4). To do so, we first extend the global boundary symmetries to the bulk as gauge symmetries, introducing the relevant bulk gauge fields. Gauged space-time symmetries require a dynamical metric, minimally described by Einstein gravity. We include a negative cosmological constant in order to get AdS asymptotics. Moreover, we add the corresponding Yang-Mills fields needed to gauge the boundary $U(2)$ symmetry, and the total action takes the form

$$S = \int d^4x\sqrt{-g}(R - 2\Lambda) - \frac{1}{4}\int [F \wedge {}^\star F + \mathrm{Tr}(G \wedge {}^\star G)], \tag{5}$$

where the last integral is defined over the AdS boundary. Here, $F = dA$ represents a $U(1)$ gauge field strength accounting for the conservation of particle number, while $G = dB - i(q/2)B \wedge B$ is the strength of a $SU(2)$ gauge field, accounting for the flavor symmetry in UV of the model in Eq. (4). One may therefore roughly state that, at this step, matter is hidden behind the black hole horizon, and an exterior observer can only see the total charges.

Hence, we look for asymptotically AdS black holes solutions, with the generic *ansatz* for the metric

$$\mathrm{d}s^2 = \frac{1}{r^2}\left(-Nf\mathrm{d}t^2 + \frac{dr^2}{f} + dx^2 + dy^2 + 2h\,dx\,dy\right), \tag{6}$$

in terms of purely r–dependent functions f, N, and h, which close to the boundary satisfy $f, N \to 1$, and $h \to 0$. To describe a boundary system at finite temperature, we focus on black hole solutions with a horizon at finite $r = r_h$, at which N and h are bounded, and f vanishes linearly with $f' = 4\pi T/\sqrt{N}$.

For the gauge fields, we write

$$A = 0$$
$$B = \frac{1}{2}(Q_1\sigma_1 + Q_2\sigma_2)dx + \frac{1}{2}(Q_1\sigma_2 + Q_2\sigma_1)\,dy. \tag{7}$$

The gauge field A, coupled at the boundary to the particle current, is turned off, implying that the chemical potential vanishes. Here $Q_{1,2}$ are the r-dependent functions which are finite at the horizon. On the boundary, we turn on a deformation analogous to the second term of the action (4), by requiring $B \to W$ or equivalently $Q_1 \to 2m_*$. This reproduces the symmetry breaking pattern of our free model in the present holographic (i.e., strongly coupled) setup. We notice at this point that a similar approach has already been used to construct holographic duals of fermions with particular dispersion relations, as, for instance, Weyl semimetals [19], multi-Weyl semimetals [11,20], nodal line semimetals [21], and Weyl Z_2 semimetals [22].

The resulting phase diagram in terms of the gauge coupling q and the dimensionless temperature T/m_* is shown in Fig. 1. At high enough T/m_* and q, only rotational invariant solutions are present, with h and Q_2 vanishing. The model flows toward a metastable Lifshitz geometry in the IR, with a scaling exponent z that is completely fixed by the coupling q, as the root of a cubic polynomial [23]

$$q^2(z^3 + z^2) + (q^2 - 24)z - 3(q^2 + 8) = 0. \tag{8}$$

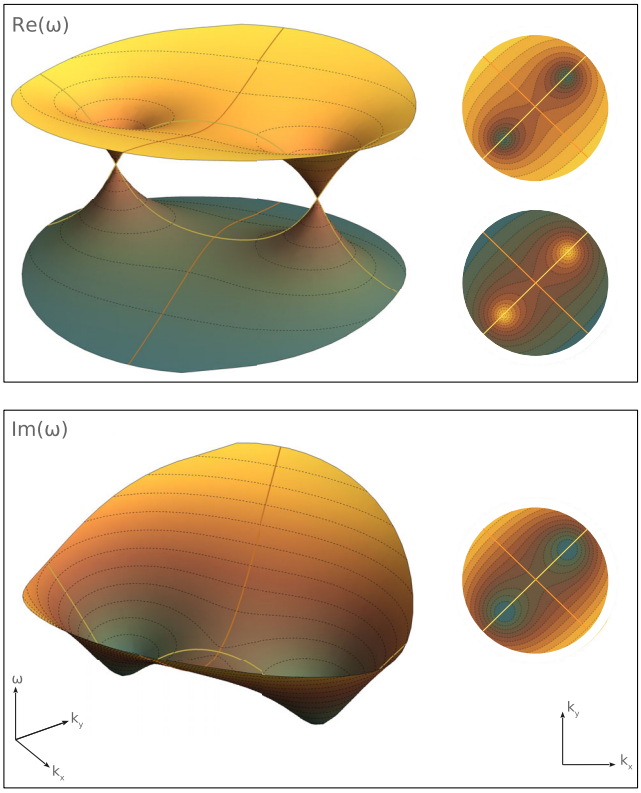

FIG. 2. Real (top panel) and imaginary (bottom panel) parts of the quasinormal frequencies for the fermionic excitations as a function of momentum $\mathbf{k} = (k_x, k_y)$ in the nematic phase, just below the critical temperature $T/m_* \approx 0.075$. The contour plots on the right hand side correspond to the 3D plots on the left. The orange and yellow lines denote the cuts which were plotted at the bottom panel of Fig. 1.

As we lower the temperature or the gauge coupling, a boundary nematic phase develops, since the fields Q_2 and h in the bulk spontaneously acquire nonvanishing expectation values. Full rotational invariance, featuring $z = 1$, is however recovered in the deep IR.

IV. FERMIONS IN THE BULK

To confirm that our holographic model actually describes flat bands, we need to obtain its fermionic dispersion relation. In holography, boundary matter fluctuations are encoded by the fermionic degrees of freedom Ψ in the bulk, satisfying the Dirac equation [24]

$$\Gamma^A D_A \Psi = 0. \tag{9}$$

Here, Γ^A with $A \in \{0, 1, 2, 3\}$ are the $(3 + 1)$-dimensional flat-space Dirac γ–matrices, and D_A is the curved space and gauge covariant derivative. The field Ψ is an $SU(2)$ doublet of $(3 + 1)$–dimensional spinors, containing a total of eight independent components.

As our model is closely related to the non-Abelian p-wave superconductor [25–30], here we only sketch the construction of D^A. The key step is to write the metric in the tetrad formalism

$$ds^2 = \eta_{AB} e^A e^B, \tag{10}$$

where $\eta_{AB} = \mathrm{diag}(-1,1,1,1)$ is the Minkowski metric and e^A are the coframe fields, given by

$$\begin{aligned} e^1 &\equiv \frac{1}{2r}[(\sqrt{1+h}+\sqrt{1-h})dx + (\sqrt{1+h}-\sqrt{1-h})\,dy], \\ e^2 &\equiv \frac{1}{2r}[(\sqrt{1+h}-\sqrt{1-h})dx + (\sqrt{1+h}+\sqrt{1-h})\,dy], \\ e^3 &\equiv \frac{1}{r\sqrt{f}}dr, \qquad e^0 \equiv \frac{1}{r}\sqrt{Nf}dt. \end{aligned} \tag{11}$$

The corresponding spin connection can be then found from the torsionless condition; for the technical details and conventions, see Ref. [31]. We furthermore conveniently perform Fourier transform from the transverse coordinates, $(t,x,y) \to (\omega, k_x, k_y)$, and rescale the spinors as

$$\Psi = r^{3/2}(fN(1-h^2))^{-1/4}\psi_k(r). \tag{12}$$

Projecting now onto the $(2+1)$–dimensional transverse spacetime by taking the eigenvectors of the radial γ–matrix, we obtain the form of the projected spinor $\psi_{\mathbf{k}}^\top = (\psi_+, \psi_-)^\top$, with the two components $\psi_\pm$ obeying the following equations:

$$\begin{aligned} \psi_-' - \frac{i}{\sqrt{2f(1-h^2)\tilde{h}}} U\cdot\psi_+ = 0, \\ \psi_+' + \frac{i}{\sqrt{2f(1-h^2)\tilde{h}}} U\cdot\psi_- = 0. \end{aligned} \tag{13}$$

Here, $\tilde{h} \equiv 1+\sqrt{1-h^2}$, $H \equiv h + i\tilde{h}$, and

$$U = \begin{pmatrix} \tilde{h}k_y - hk_x & \tilde{h}k_x - hk_y + \sqrt{\frac{2(1-h^2)\tilde{h}}{fN}}\omega & \frac{1}{2}q_D(HQ_1 - iH^*Q_2) & \frac{1}{2}q_D(HQ_2 - H^*Q_1) \\ \tilde{h}k_x - hk_y + \sqrt{\frac{2(1-h^2)\tilde{h}}{fN}}\omega & hk_x - \tilde{h}k_y & \frac{1}{2}q_D(HQ_2 - iH^*Q_1) & \frac{1}{2}q_D(H^*Q_1 + iH^*Q_2) \\ \frac{1}{2}q_D(H^*Q_1 + iHQ_2) & \frac{1}{2}q_D(-iH^*Q_1 - H^*Q_2) & \tilde{h}k_y - hk_x & \tilde{h}k_x - hk_y + \sqrt{\frac{2(1-h^2)\tilde{h}}{fN}}\omega \\ \frac{1}{2}q_D(-iHQ_1 + H^*Q_2) & \frac{1}{2}q_D(-H^*Q_1 - iHQ_2) & \tilde{h}k_x - hk_y - \sqrt{\frac{2(1-h^2)\tilde{h}}{fN}} & hk_x - \tilde{h}k_y \end{pmatrix}. \tag{14}$$

Close to the boundary, the fields $\psi_\pm$ are asymptotically constant, $\psi_\pm \to \psi_\pm^{\mathrm{UV}}$. The four components of ψ_+^{UV} are interpreted as the expectation values of the dual fermionic operator, while those of ψ_-^{UV} are instead proportional to the external sources. On the other hand, close to the black hole horizon, in-going boundary conditions yield

$$\psi_\pm = \psi_{h\pm}(r-r_h)^{-\frac{i\omega}{4\pi T}} \tag{15}$$

with $\psi_{h+} = -i(I_{2\times 2}\otimes\sigma_2)\cdot\psi_{h-}$. This constraint implies that $\psi_\pm^{\mathrm{UV}}$ are not all independent. Indeed, since the equations are linear, we can assume the linear relations $\psi_+^{\mathrm{UV}} = M_+\psi_h$ and $\psi_-^{\mathrm{UV}} = M_-\psi_h$, where the matrices $M_\pm$ must be obtained by numerical integration. This in turn implies $\psi_+^{\mathrm{UV}} = M_+M_-^{-1}\psi_-^{\mathrm{UV}}$, allowing us to identify the retarded fermionic correlator as $G = M_+M_-^{-1}$. Then the poles of the correlator can be simply read off from the zeros of the determinant of M_-. Notice that in contrast to previous construction [32], in our model we apply the standard relativistic boundary conditions and the flatness of the bands arises from the bulk dynamics.

V. FERMIONIC DISPERSION RELATION

Focusing on the lowest lying poles of the previously discussed retarded correlator, we obtain the dispersion relation of the holographic fermion. Starting at the infinite temperature limit, its form reads

$$\omega \approx -i + v_f k - i\Gamma k^2 + \ldots \tag{16}$$

featuring a purely imaginary gap and a real part scaling linearly with k, as expected for a massless fermion. At large k nonlinear contributions coming from the broken conformal symmetry have to be included. The corresponding dispersions are shown at the top panel of Fig. 1.

As the temperature is lowered, the fermionic dispersion relation in Eq. (16) gets modified to

$$\omega \approx -i + ck^2 - i\Sigma k^4 + \ldots \tag{17}$$

in agreement with expectations based on the free model. This can be seen in the plots at the right panel of Fig. 1. We emphasize that the dispersion relation in Eq. (17) fits to a

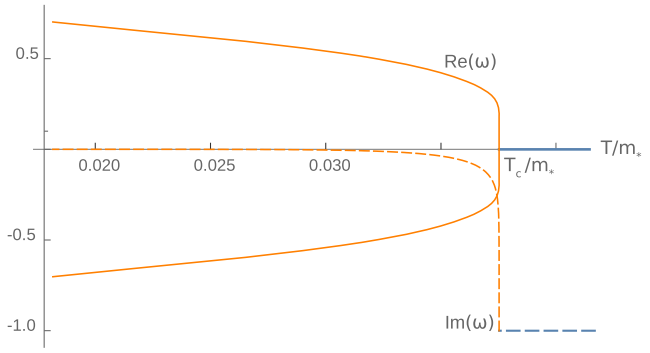

FIG. 3. Real and imaginary part of the quasinormal frequencies at $\mathbf{k} = 0$ for the fermionic excitations as a function of the temperature for the nematic phase (orange) and the flat bands phase (blue).

quadratic real part close enough to the origin. This behavior holds until the system enters the instability toward the nematic phase, where the dispersion relation becomes direction dependent. To illustrate this behavior, two representative cuts along the diagonal and antidiagonal directions in the $\mathbf{k}$–plane are shown at the bottom panel of Fig. 1. We observe a rather notable breaking of the rotational invariance. Interestingly, a zero frequency excitation at a finite $k = k_*$ along one of the directions shows up yields a relativistic behavior in its vicinity. This is a consequence of a $z = 1$ fixed point, which corresponds to the deep IR of the zero temperature limit in the nematic phase.

Additionally, in Fig. 2 we show a 3D plot with the position of the poles of the two point function in the momentum space. We see explicitly that rotational symmetry is broken while a discrete Z_2 symmetry around the $k_x + k_y$ axis is preserved. As we can see in Fig. 3 the real part of the zero momentum quasinormal frequency quickly grows for the nematic phase, while the imaginary part drops to zero. These gaps lift the degeneracy at low energies according to the expected instability of flat bands in interacting systems. On the other hand, the imaginary part drops to zero, making otherwise incoherent fermionic quasiparticle excitations long lived as the temperature is lowered.

VI. CONCLUSIONS AND OUTLOOK

In this paper, we realized a construction of fermionic flat bands in the context of holography by directly including the fermions in the bulk geometry within a standard bottom-up approach. We consider a holographic system inspired by a free fermionic model that mimics two copies of Dirac fermions hybridizing as in a graphene bilayer and yielding a quadratic low-energy dispersion. Interestingly, we found that the holographic fermions inherit this quadratic dispersion relation from the free model, while the thermodynamics of the system points toward a different Lifshitz exponent. This should not be surprising given that the holographic system is strongly coupled with the strongly renormalized critical exponents, which is then encoded in the scaling of the thermodynamic response functions.

We here point out that since a holographic system is intrinsically strongly coupled, and, on the other hand, a flat electronic band is highly degenerate, we expect that the holographic flat band undergoes a phase transition toward a phase where the degeneracy is lifted. This is in fact consistent with the present holographic setup, since the Yang-Mills black holes, featured in the model, are generically unstable. This fact is reflected as a phase transition toward a nematic phase. The concomitant rotational symmetry breaking then leads to the splitting of the quadratically dispersing nodes into two relativistic Dirac points that move apart as we lower the temperature. As such, this process can be thought as a holographic realization of the Berry monopole splitting at strong coupling.

We emphasize that our model contains the minimal ingredients required by a holographic construction, i.e., Einstein gravity with a negative cosmological constant and a Yang-Mills field gauging the boundary global symmetries. Our results should therefore hold also in more general models realizing flat bands holographically, with a similar symmetry breaking pattern. As a consequence, we expect that the emergence of a nematic phase at low temperatures represents a ubiquitous feature of flat bands at strong coupling. This nematic phase implies a richer fermionic content which should be responsible for the form of the anomalous Hall effect, as reported in Ref. [10]. In turn, one may consider this observable as a benchmark imprint for the Berry monopole splitting in the conductivity.

We also point out that the nematic phase we found in our holographic model shows some qualitatively similar features as the one recently observed in twisted double bilayer graphene [33], such as the breaking of the rotational symmetry down to the Z_2 subgroup while preserving the translational one. These properties can be seen directly from the quasinormal mode spectrum in Fig 1. Additionally, we predict that the nematic phase should exhibit anomalous Hall conductivity, with the qualitative form as in Figs. 7 and 8 in Ref. [10].

As for the future directions, one may consider a UV completion of our bottom-up model where the relation between the bosonic and fermionic sector arises from a stringy construction [34–37]. Furthermore, the free fermionic construction can be extended to an arbitrary integer n with the dispersion $\omega \sim k^n$ by using n fermionic flavors and the generators of the spin-$(n-1)/2$ representation of the $SU(2)$ group [11]. It would be therefore interesting to investigate holographic duals of the models with higher-n fermionic dispersions. Finally, one may explore generalizations of these fermionic models to non-relativistic Goldstone bosons [38,39].

ACKNOWLEDGMENTS

This work was supported by ANID-SCIA ANILLO Grant No. ACT210100 (R. S.-G. and V. J.), the Swedish Research Council Grant No. VR 2019-04735 (V. J.), Fondecyt (Chile) Grant No. 1200399 (R. S.-G.), the CONICET Grants No. PIP-2017-1109 and No. PUE 084 "Búsqueda de Nueva Física", and by UNLP Grant No. PID-X791 (I. S. L. and N. E. G.).

[1] Y. Cao, V. Fatemi, A. Demir, S. Fang, S. L. Tomarken, J. Y. Luo, J. D. Sanchez-Yamagishi, K. Watanabe, T. Taniguchi, E. Kaxiras *et al.*, Nature (London) **556**, 80 (2018).
[2] Y. Cao, V. Fatemi, S. Fang, K. Watanabe, T. Taniguchi, E. Kaxiras, and P. Jarillo-Herrero, Nature (London) **556**, 43 (2018).
[3] E. Y. Andrei and A. H. MacDonald, Nat. Mater. **19**, 1265 (2020).
[4] J. M. Maldacena, Adv. Theor. Math. Phys. **2**, 231 (1998).
[5] E. Witten, Adv. Theor. Math. Phys. **2**, 253 (1998).
[6] M. Ammon and J. Erdmenger, *Gauge/Gravity Duality: Foundations and Applications* (Cambridge University Press, Cambridge, England, 2015).
[7] J. Zaanen, arXiv:2110.00961.
[8] S. A. Hartnoll, A. Lucas, and S. Sachdev, *Holographic Quantum Matter* (MIT Press, Cambridge, MA, 2018).
[9] J. Zaanen, Y. Liu, Y.-W. Sun, and K. Schalm, *Holographic Duality in Condensed Matter Physics* (Cambridge University Press, Cambridge, England, 2015).
[10] N. Grandi, V. Juričić, I. Salazar Landea, and R. Soto-Garrido, J. High Energy Phys. 05 (2021) 123.
[11] R. M. Dantas, F. Peña-Benitez, B. Roy, and P. Surówka, Phys. Rev. Research **2**, 013007 (2020).
[12] B. Wunsch, F. Guinea, and F. Sols, New J. Phys. **10**, 103027 (2008).
[13] G. Montambaux, F. Piéchon, J.-N. Fuchs, and M. O. Goerbig, Phys. Rev. B **80**, 153412 (2009).
[14] L. Tarruell, D. Greif, T. Uehlinger, G. Jotzu, and T. Esslinger, Nature (London) **483**, 302 (2012).
[15] C. Zhang *et al.*, Nat. Phys. **13**, 979 (2017).
[16] B. Roy, P. Goswami, and V. Juričić, Phys. Rev. B **95**, 201102 (2017).
[17] I. Belopolski, T. A. Cochran, X. Liu, Z.-J. Cheng, X. P. Yang, Z. Guguchia, S. S. Tsirkin, J.-X. Yin, P. Vir, G. S. Thakur, S. S. Zhang, J. Zhang, K. Kaznatcheev, G. Cheng, G. Chang, D. Multer, N. Shumiya, M. Litskevich, E. Vescovo, and T. K. Kim *et al.*, Phys. Rev. Lett. **127**, 256403 (2021).
[18] G. G. Liu *et al.*, arXiv:2106.02461.
[19] K. Landsteiner and Y. Liu, Phys. Lett. B **753**, 453 (2016).
[20] V. Juričić, I. Salazar Landea, and R. Soto-Garrido, J. High Energy Phys. 07 (2020) 052.
[21] Y. Liu and Y.-W. Sun, J. High Energy Phys. 12 (2018) 072.
[22] X. Ji, Y. Liu, Y.-W. Sun, and Y.-L. Zhang, J. High Energy Phys. 12 (2021) 066.
[23] D. O. Devecioğlu, Phys. Rev. D **89**, 124020 (2014).
[24] M. Henningson and K. Sfetsos, Phys. Lett. B **431**, 63 (1998).
[25] S. S. Gubser and S. S. Pufu, J. High Energy Phys. 11 (2008) 033.
[26] M. Ammon, J. Erdmenger, M. Kaminski, and P. Kerner, Phys. Lett. B **680**, 516 (2009).
[27] M. Ammon, J. Erdmenger, V. Grass, P. Kerner, and A. O'Bannon, Phys. Lett. B **686**, 192 (2010).
[28] R. E. Arias and I. S. Landea, J. High Energy Phys. 01 (2013) 157.
[29] S. S. Gubser, F. D. Rocha, and A. Yarom, J. High Energy Phys. 11 (2010) 085.
[30] M. Ammon, J. Erdmenger, M. Kaminski, and A. O'Bannon, J. High Energy Phys. 05 (2010) 053.
[31] G. L. Giordano, N. E. Grandi, and A. R. Lugo, J. High Energy Phys. 04 (2017) 087.
[32] J. N. Laia and D. Tong, J. High Energy Phys. 11 (2011) 125.
[33] C. Rubio-Verdu, S. Turkel, Y. Song *et al.*, Nat. Phys. **18**, 196 (2022).
[34] J. L. Davis, H. Omid, and G. W. Semenoff, J. High Energy Phys. 09 (2011) 124.
[35] G. Grignani, N. Kim, A. Marini, and G. W. Semenoff, J. High Energy Phys. 12 (2014) 091.
[36] M. Ammon, J. Erdmenger, M. Kaminski, and P. Kerner, J. High Energy Phys. 10 (2009) 067.
[37] K. Bitaghsir Fadafan, A. O'Bannon, R. Rodgers, and M. Russell, J. High Energy Phys. 04 (2021) 162.
[38] I. Amado, D. Arean, A. Jimenez-Alba, K. Landsteiner, L. Melgar, and I. S. Landea, J. High Energy Phys. 07 (2013) 108.
[39] T. Schäfer, D. T. Son, M. A. Stephanov, D. Toublan, and J. J. M. Verbaarschot, Phys. Lett. B **522**, 67 (2001).